Isobaric-Analog Study of ^{90}Zr†

K. P. Lieb,* James J. Kent, and C. Fred Moore
University of Texas at Austin, Austin, Texas 78712
(Received 6 June 1968)

Proton-induced analog resonance reactions have been studied using the target ^{90}Zr. Excitation functions were measured for elastic and inelastic protons at angles of 70°, 110°, 130°, 150°, and 170°. The inelastic groups detected result from the 0^+ (1.75-MeV), 2^+ (2.18-MeV), 5^- (2.32-MeV), and the unresolved 4^- and 3^- (2.75-MeV) states in ^{90}Zr. In addition, proton inelastic angular distributions have been taken on and off the more prominent resonances. In order to separate the resonances attributed to the 4^- and 3^- (2.75-MeV) proton group, excitation of the 4^- to 5^- and 3^- to 2^- γ rays were measured in a 26-cm^3 Ge(Li) detector.

1. INTRODUCTION

THIS paper contains the results of an investigation of analog resonances in the ^{90}Zr plus proton system. The incident proton energy ranged from 6.1 to 9.6 MeV, which corresponds to excitation energies of 11.4 to 14.9 MeV in the compound nucleus ^{91}Nb (B_p=5.27 MeV). The resonances in this region are analogs of the excited states of ^{91}Zr, as has previously been demonstrated[1] by elastic scattering.

Elastic scattering data taken over isobaric analog resonances (IAR) yield information similar to that obtained from (d,p) reactions on the ground state of ^{90}Zr leading to the various states in ^{91}Zr where the overlap of these final states with a single neutron coupled to the ground state of ^{90}Zr is measured. Inelastic scattering over analog resonances yields similar information on excited states of the target. Assuming a single-particle model for ^{91}Zr, the parent analog states are written as

$$\psi_{\mathrm{PA}}{}^m(^{91}\mathrm{Zr})=\sum_{klj} b_{km}{}^{lj}\phi_c{}^k\nu(l_j)\,, \tag{1}$$

where $\phi_c{}^k$ denotes the orthogonal, normalized set of ^{90}Zr states ($\phi_c{}^0$=ground state) and $\nu(l_j)$ denotes the valence neutron state. (In the case of pure shell-model configurations for core plus single particle with the residual interaction neglected, the $b_{km}{}^{lj}$ are essentially the coefficients of fractional parentage.) The $T_>$ part of the IAR is obtained by setting

$$\psi_A{}^m(^{91}\mathrm{Nb})=T^-\psi_{\mathrm{PA}}{}^m(^{91}\mathrm{Zr})=\sum_{klj}\frac{b_{km}{}^{lj}}{(2T_0+1)^{1/2}}\times[\phi_c{}^k\pi(l_j)+(2T_0)^{1/2}(T^-\phi_c{}^k)\nu(l_j)]\,, \tag{2}$$

where $\pi(l_j)$ stands for the single proton wave function. If isospin mixing is neglected the partial width $\Gamma_0{}^{lj}$ in the incoming channel is given by

$$\Gamma_0{}^{lj}\propto|b_{0m}{}^{lj}|^2/(2T_0+1)\,.$$

The width in an inelastic channel $k\neq0$,

$$\Gamma_k{}^{lj}\propto|b_{km}{}^{lj}|^2/(2T_0+1)\,,$$

contains two parts: one from the "weak-coupling" part $\phi_c{}^k\pi(l_j)$ and one from the 2p−1h part $(T^-\phi_c{}^k)\nu(l_j)$. It has been pointed out[2] in the case of a ^{88}Sr target that the latter contribution is much smaller than the former one for populating the lowest 2^+ and 3^- collective states in ^{88}Sr. The level scheme of ^{90}Zr includes single-particle states at 1.75 MeV (0^+), 2.32 MeV (5^-) and 2.75 MeV (4^-) besides the 2^+ and 3^- collective states at 2.18 and 2.75 MeV, respectively. It is the scheme of this experiment to investigate the application of the above description to the ^{90}Zr+p system.

2. EXPERIMENTAL METHODS AND RESULTS

A. Excitation Curves of Proton Groups

The incident proton beam used in this experiment was obtained from the EN tandem Van de Graaff accelerator at The University of Texas at Austin. The target was a ^{90}Zr foil of 97.8% purity obtained from ORNL Separated-Isotopes Division. The measured thickness of the target was 0.57 mg/cm^2, as determined by Rutherford scattering. The scattered protons were observed by solid-state detectors placed at laboratory scattering angles of 70°, 110°, 130°, 150°, and 170° in an 18-in. scattering chamber. The detectors were cooled by dry ice and methanol placed in a cold trap in the center of the lid of the scattering chamber.

A PDP-7 computer was used as a multichannel analyzer with 1024 channels for each detector. A beam of about 0.1 μA was maintained, and an integrated beam current of 50 μC was collected for each data point. The current integrator was connected with the computer to correct for dead time. A sample spectrum is shown in Fig. 1.

Excitation curves were obtained for scattering to the ground state (0^+) and several low-lying excited states of ^{90}Zr: 1.75 MeV (0^+), 2.18 MeV (2^+) and 2.75 MeV (3^-,4^-). The 3^- and 4^- states could not be resolved in the proton spectrum (see Sec. 2 C). The proton group

† Supported in part by the U. S. Atomic Energy Commission and by the Robert Welch Foundation (Grant F-166).
* Fulbright Fellow.
[1] C. F. Moore, thesis, Florida State University, 1964 (unpublished); J. J. Kent, thesis, University of Texas at Austin, 1967 (unpublished).
[2] N. Auerbach, Phys. Letters **27B**, 127 (1968).

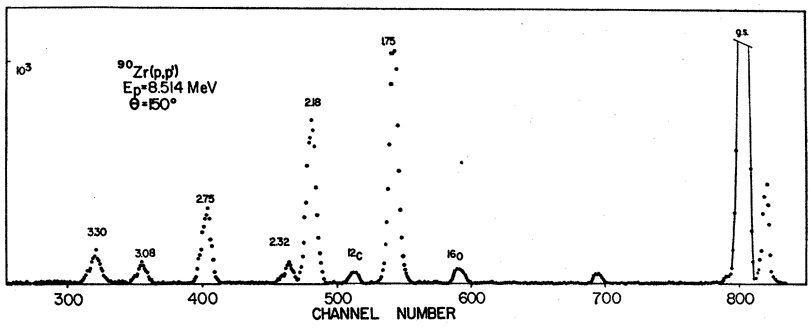

FIG. 1. Proton spectrum of the reaction ^{90}Zr(p,p') at 8.514-MeV bombarding energy and 150° laboratory angle.

from the 2.32-MeV (5^-) state was generally quite small and not completely resolved from the proton group corresponding to the 2.18-MeV state. Gaps in some of the excitation curves are due to the ^{12}C impurity peak passing through the observed peak.

The excitation curves for elastic scattering at the five observed scattering angles covering the range from 6.1 to 9.5 MeV bombarding energy are shown in Fig. 2. The observed anomalies have been identified as the isobaric analogs of several low-lying states in ^{91}Zr. The energies and spins for the ^{91}Zr states are known from the ^{90}Zr(d,p)^{91}Zr experiment of Cohen and Chubinsky.[3] The analogs of the $d_{5/2}$ ground state and $s_{1/2}$ (1.21-MeV) state lie below the energy range covered in this experiment, but have been observed previously.[1,4]

The excitation curves for inelastic scattering leading to the $0^+,2^+$ and $3^-,4^-$ states are shown in Figs. 3–5. A 150° excitation function of the 5^- inelastic group taken in a previous experiment[1] is shown in Fig. 6. All of the excitation curves show a number of resonances, frequently at an energy where only a small resonance is seen in the elastic scattering excitation curves.

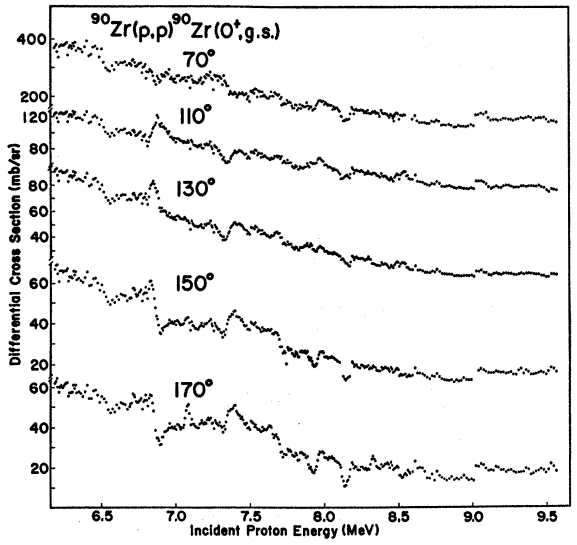

FIG. 2. Excitation functions at 70°, 110°, 130°, 150°, and 170° of the elastic scattering proton group.

[3] B. L. Cohen and O. V. Chubinski, Phys. Rev. **131**, 2184 (1963).
[4] C. F. Moore, S. A. A. Zaidi, and J. J. Kent, Phys. Rev. Letters **18**, 345 (1967).

B. Angular Distributions of Proton Groups

Angular distributions from 45° to 170° in 5° steps were taken on and off a number of the resonances seen in the inelastic excitation curves. The stability of the beam was checked by counting the elastically scattered protons in a 90° monitor detector. A smaller range of angles was covered by a second rotating detector. At forward angles the background coming from the tail of the elastic scattering peak was subtracted. Below 50° an additional deadtime correction of 7% was necessary. The results for off-resonance elastic scattering are shown in Fig. 7 and those for inelastic scattering are shown in Fig. 8. Each angular distribution in Fig. 8 is labeled by the incident proton energy and the expected weak-coupling structure. The large errors in the cross-section measurements at some of the backward angles are due to the fact that the ^{12}C impurity peak passed through the inelastic proton peak at those angles. Except for the $s_{1/2}$ resonance at 7.34 MeV, all angular distributions of the p_1 group are remarkably

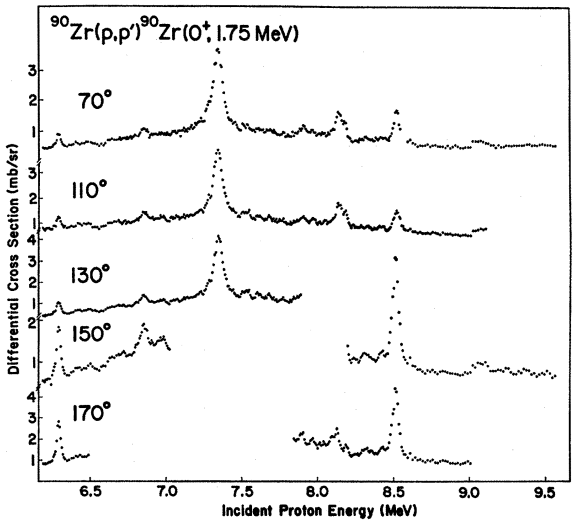

FIG. 3. Inelastic scattering excitation functions of the p_1 (0^+) 1.75-MeV proton group.

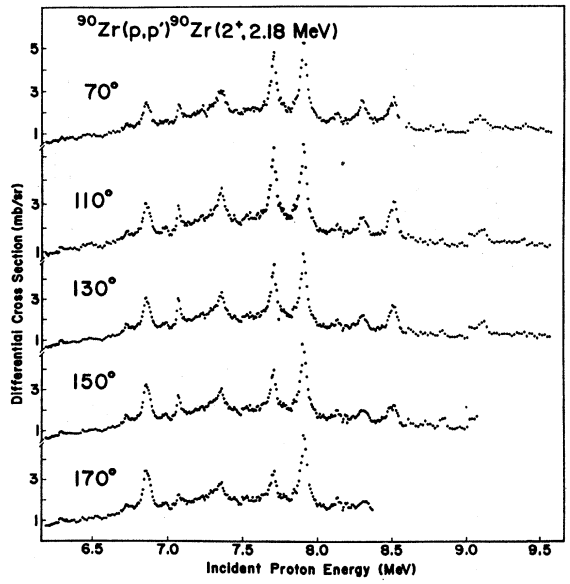

FIG. 4. Inelastic scattering excitation functions of the p_2 (2^+) 2.18-MeV proton group.

symmetric around 90°, showing a strong P_2 term. The angular distributions of the p_2 group [Fig. 8(b)] on the other hand, do not show fore-aft symmetry, but are rather smooth.

C. Measurements of ^{90}Zr($p,p_{3^-,4^-}$) γ Rays

It is known from experiments on ^{138}Ba (Ref. 5) and ^{208}Pb (Ref. 6) targets that inelastic proton scattering

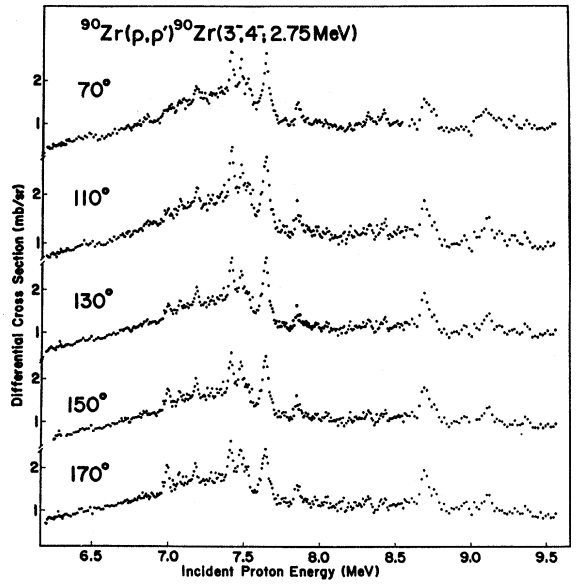

FIG. 5. Inelastic scattering excitation functions of the $p_{4,5}$ (3^-, 4^-) 2.75-MeV proton doublet.

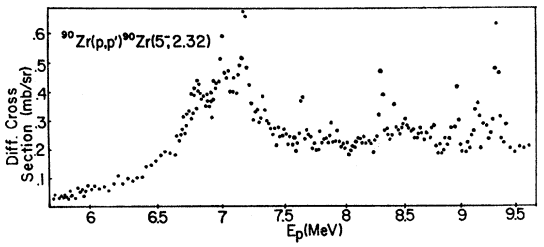

FIG. 6. Inelastic scattering excitation functions of the p_3 (5^-) 2.32-MeV proton group.

through IAR feeding the lowest-octupole vibrational state gives information on its neutron 1p–1h structure. The excitation function of the $p_{4,5}(3^-,4^-)$ group in ^{90}Zr(p,p') exhibits four strong and at least eight minor resonances in the range of 6.1–9.5-MeV bombarding energy (Fig. 6). In order to separate the resonances of the 3^- state from those of the 4^- state, the different γ decays of the two states have been investigated. Hendrie and Farwell[7] observed that the 3^- state de-excites to the 2.18-MeV 2^+ level whereas the 4^- state decays to the

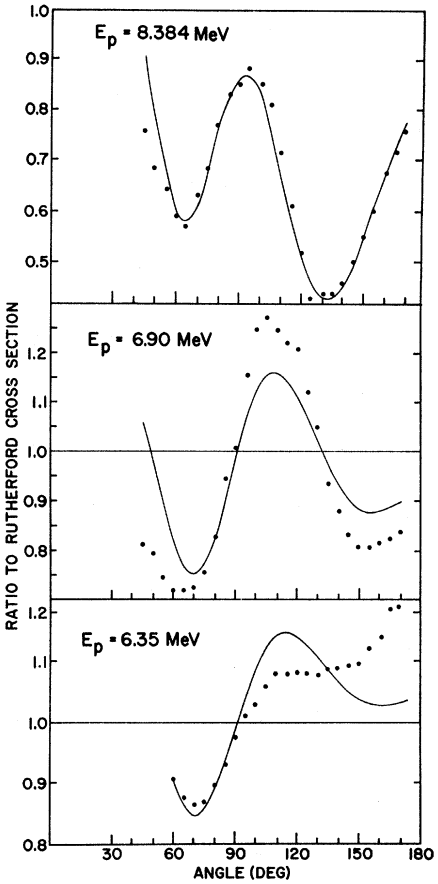

FIG. 7. Off-resonance angular distributions of elastic scattering groups at 6.35, 6.89, and 8.38 MeV, compared with Rutherford cross section. The fitting curves are obtained by the program PEREY using the optical-potential parameters listed in Table III.

[5] G. C. Morrison, N. Williams, J. A. Nolen, D. von Ehrenstein, Phys. Rev. Letters **19**, 592 (1967).

[6] C. F. Moore, L. J. Parish, P. von Brentano, and S. A. A. Zaidi, Phys. Letters **22**, 616 (1966).

[7] P. L. Hendrie and G. W. Farwell, Phys. Letters **9**, 321 (1964).

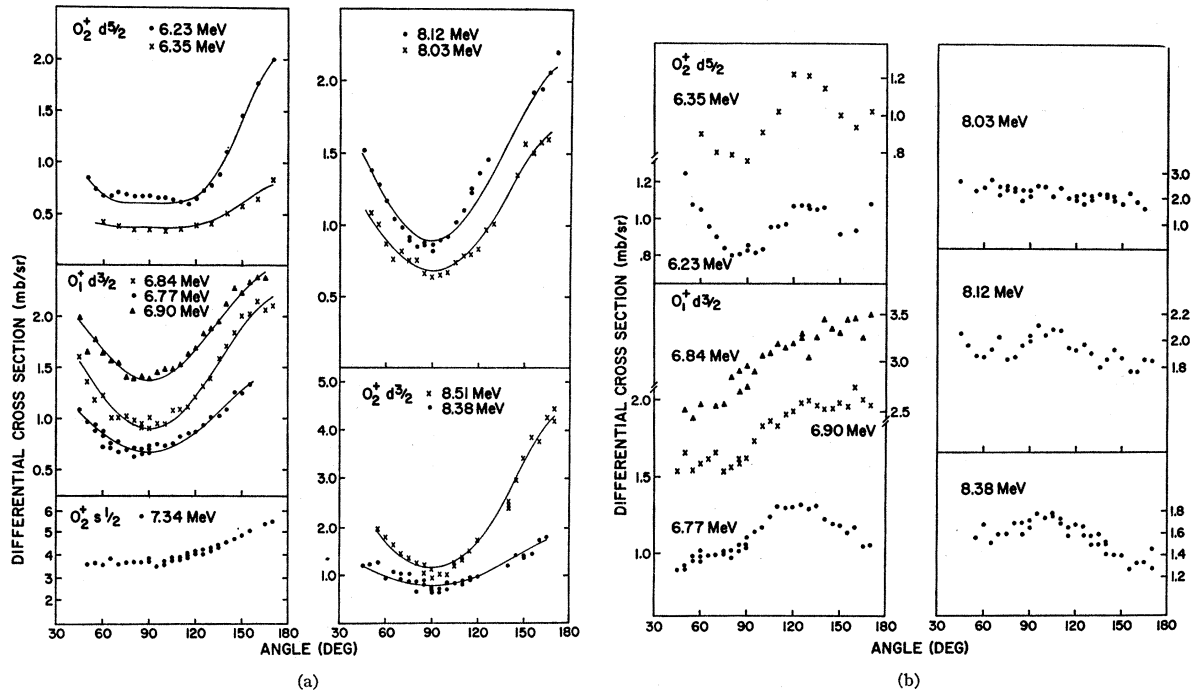

FIG. 8. (a) Angular distributions of the p_1 (0_2^+) group fitted by the expression $d\sigma(\theta)/d\Omega=(\sigma/4\pi)(1+B_2P_2+B_4P_4)$. The B_2 and B_4 coefficients are given in Table IV. (b) Angular distributions of the p_2 (2^+) group.

2.32-MeV 5^- state. Fortunately, γ-ray cascades following the ^{90}Zr$(p,n)^{90}$Nb$(\beta^+)^{90}$Zr* reaction do not involve the doublet,[8,9] nor is it populated by transitions from higher states which are weakly excited in inelastic scattering.

A 26-cm^3 Ge(Li) detector was placed 18 cm from the target and at 90° relative to the beam, which was stopped 2.5 m behind the target on a tantalum disk. The detector was shielded against background radiation from the stopper by a 60-cm-thick concrete wall and from the beam-defining slits by a 7-cm-thick lead collimator. A 1-cm steel plate in front of the detector reduced the low-energy γ counting rate and the dead-time losses of the system and improved the energy resolution. Part of a spectrum taken in the 7.35-MeV resonance is displayed in Fig. 9. From a calibration of several spectra including some of the ^{90}Nb activity, the excitation energies listed in Table I have been found to be in good agreement with a recent ^{90}Nb β^- decay study.[9] The energies of the states in the 2.74-MeV doublet are found to be 2742±1 keV (3^-) and 2748±1 keV (4^-), respectively.

Excitation functions of the $4^- \rightarrow 5^-$ and $3^- \rightarrow 2^+$ γ rays have been measured in 20-keV steps at bombarding energies about those where the $p_{4,5}$ group was found to resonate. Figure 10 shows an excitation curve of the integrated full energy peaks covering the three strong resonances near 7.5 MeV. They correspond well to the 70° $p_{4,5}$ data given in the lowest part of the figure. Be-

TABLE I. Energies of lowest excited states in ^{90}Zr

J^π	Excitation energy (keV) Present work	[a]	[b]
0^+	···	1750	1760.7 ±0.6
2^+	2187±1	2182	2186.2 ±0.4
5^-	2319±1	2315	2318.69±0.18
3^-	2742±1	2745	···
4^-	2748±1	···	···
4^+	···	3081	3076.8 ±0.5
2^+	3308±1.5	3310	···
6^+	3449±1.5	3453	3447.78±0.34
8^+	···	3595	3589.03±0.31

[a] Reference 8.
[b] Reference 9.

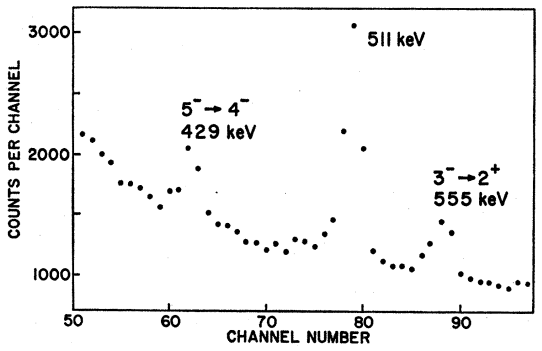

FIG. 9. Part of the Ge(Li) spectrum of the ^{90}Zr$(p,p'\gamma)$ reaction at 7.35 MeV.

[8] S. B. Bjornholm *et al.*, Phys. Rev. **115**, 1613 (1959).
[9] H. Petterson, S. Arntmann, and Y. Grunditz, Nucl. Phys. **A108**, 124 (1968).

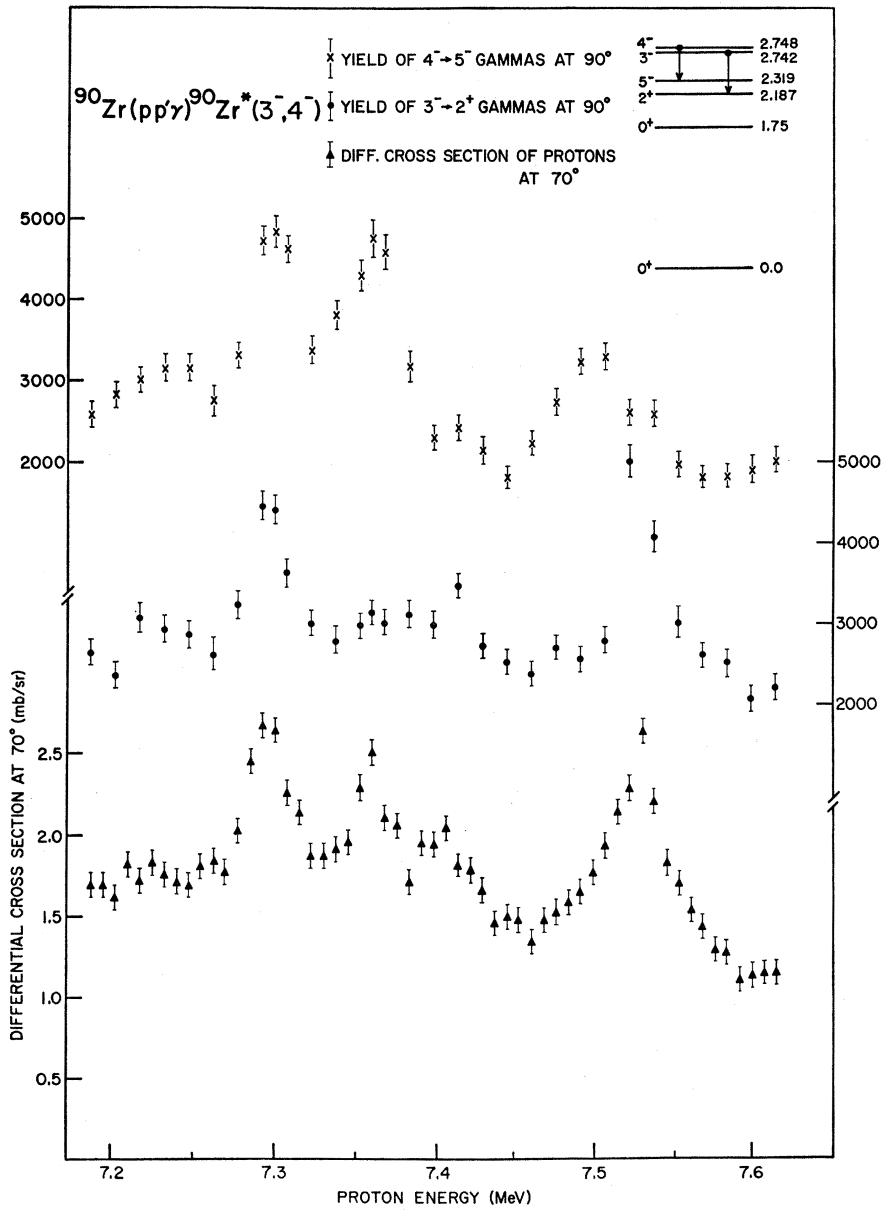

FIG. 10. Yield curves of the $4^- \rightarrow 5^-$ and $3^- \rightarrow 2^+$ γ rays covering the three strong resonances near 7.4 MeV.

cause of the increasing neutron yield from the $^{90}Zr(p,n)$ reaction above 7.56 MeV, the γ-ray spectrum deteriorates so that the $4^- \rightarrow 5^-$ 429-keV line is not well separated from the background. In addition, inelastic neutron scattering on the ^{76}Ge isotope within the detector produces 563-keV radiation which obscures the $3^- \rightarrow 2^+$ 555-keV line.[10] Nevertheless, it was still possible to relate resonances at 8.27, 8.37, and 8.63 MeV in both the $p_{4,5}$ and $3^- \rightarrow 2^+$ γ-ray excitation functions.

D. $^{90}Zr(p,n)$ Threshold

In order to extract resonance parameters of the IAR from the (p,p_0) and (p,p') data, one needs to determine the contributions to the cross section from the $T_<$ states, which are usually described in terms of an optical model. It has been obvious from the analysis of the $Y^{89}(p,n)Zr^{89}$ reaction near the (p,n) threshold[11] and of the $^{90}Zr(p,p_0)$ reaction below the (p,n) threshold[12] that a standard set of optical parameters provides much too large an estimate for the imaginary part of the optical potential which, on the other hand, is expected to rise above the threshold.

A rough search for the effective threshold energy of the $Zr^{90}(p,n)Nb^{90}$ channel has been made by looking at

[10] C. Chasman, Nucl. Instr. Methods 37, 1 (1965).

[11] C. H. Johnson, P. L. Kernell, and S. Ramavataram, Nucl. Phys. A107, 21 (1968).

[12] W. J. Thompson, J. L. Adams, and D. Robson, Phys. Rev. (to be published).

the buildup of Nb^{90} activity. The β^+ decay of the Nb^{90} 8^+ ground state is[8,9,13] followed by the 3.589 $(8^+) \rightarrow$ 3.449 $(6^+) \rightarrow$ 2.319 $(5^-) \rightarrow$ ground-state γ-ray cascade in Zr^{90}. Since both the 6^+ and 8^+ state in Zr^{90} are only weakly excited in the inelastic scattering process, the clearly resolved $6^+ \rightarrow 5^-$ 1130-keV transition measures the activity.

A serious disadvantage of this method results from the long lifetime $\tau = 15$ h of Nb^{90}, which restricts the measurements to the vicinity of the threshold. The excitation curve of the $6^+ \rightarrow 5^-$ γ rays has been measured simultaneously with the $(p,p_{4,5})$ γ rays for the bombarding energy increasing from 7.30 to 7.70 MeV. The yield curve is given in Fig. 11(a); it shows a sharp jump near 7.56 ± 0.08 MeV corresponding to the threshold of the states in Nb^{90} near 560 ± 80 keV. As the ground state $(J^\pi = 8^+)$ and the 122-keV doublet $(J^\pi = 6^+$ and $4^-)$ are not populated due to the high partial waves required, likely candidates for the source of the activity are the 326- (3^-), 380- (1^+), 446- (3^-) and 488-keV (2^-) states.[14] The data favor the 488-keV state, though correction for the increasing amount of activity would lower the slope of the step so that the 446-keV state cannot be excluded.

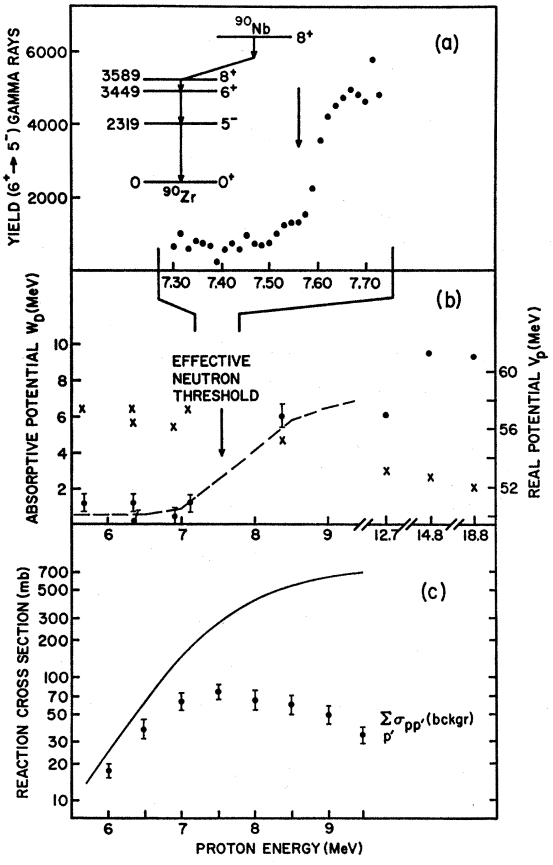

FIG. 11. (a) Excitation curve of the $6^+ \rightarrow 5^-$ γ-ray yield over the effective ^{90}Zr$(p,n)^{90}$Nb threshold at 7.56 MeV. (b) Real part $V_p(\times)$ and imaginary part $W_D(\bullet)$ of the optical-model potential are given as a function of bombarding energy. For more details refer to Table III. The dotted line has been used to calculate the background in the p_0 (0^+) and p_1 (0^+) channels. (c) The observed background cross section summed over the 0_2^+, 2^+, 5^-, 4^-, 3^- inelastic channels is compared with the total absorption cross-section line calculated with the optical potential given above. The difference below 7.5 MeV is assumed to be due to re-emission in the elastic channel.

[13] K. E. G. Löbner, Nucl. Phys. 58, 45 (1964).

3. ANALYSIS

A. Elastic Scattering Channel

Two of the main purposes for studying IAR are to deduce spectroscopic factors of the pC and nC systems and to investigate the isospin mixing of the $T_<$ background states into the $T_>$ part of the IAR. Expressions for the S matrix for elastic scattering

$$\langle S_{cc} \rangle = S_{cc}^{\text{opt}} + S_{cc}^{\text{res}}$$

averaged over the fine structure of the resonance have been derived by several authors. Here, S_{cc}^{opt} denotes the optical-potential scattering by the background states. The resonance is described by S_{cc}^{res}, which is modified by the presence of the $T_<$ states and depends on their microscopic structure. The analysis given here follows a modified approach of Weidenmüller and Mahaux,[15,16] mainly because their approach provides consistent formulas for the inelastic channels. In this theory the S matrix has the form

$$S_{cc'}^{\text{opt}} = \exp(2i\xi_{lj}) \frac{1 - Y_{lj}}{1 + Y_{lj}} \delta_{cc'}, \tag{3a}$$

$$S_{cc'}^{\text{res}} = i \exp(+i\xi_{lj} + i\xi_{l'j'}) \frac{(\Gamma_{lj}^{(A)} \Gamma_{l'j'}^{(A)})^{1/2} f_{lj} f_{l'j'}}{E - \bar{E} - \Delta + i\Gamma/2}, \tag{3b}$$

$$f_{lj} = (1 + 2iY_{lj}\Delta_{lj}^{(\text{sp})}/\Gamma_{lj}^{(\text{sp})})(1 + Y_{lj})^{-1}, \tag{3c}$$

where all other quantities are defined in Ref. 16. The spectroscopic factor of the isobaric analog resonance

$$S_p = \Gamma_{lj}^{(A)}/\Gamma_{lj}^{(\text{sp})}$$

is defined as the ratio of the proton partial width of the resonance $\Gamma_{lj}^{(A)}$ and the single-particle width[17,18]

$$\Gamma_{lj}^{(\text{sp})} = (k_p/E_p) T_0 \langle \phi_{nA} | U_1 | \phi_{pC}^{(+)} \rangle^2. \tag{4}$$

In deriving Eq. (3), Weidenmüller made the restrictive assumption that the real part of the optical proton potential V_p of the pC system and the neutron potential V_n of the nC system are equal. In recent studies of IAR built on ^{208}Pb,[17] ^{88}Sr,[19] ^{90}Zr,[12] and some $N = 82$ nuclei,[20]

[14] H. Petterson, G. Backstrom, and C. Bergmann, Nucl. Phys. 83, 33 (1966).
[15] C. Mahaux and H. A. Weidenmüller, Nucl. Phys. A93, 327 (1967).
[16] H. A. Weidenmüller, Nucl. Phys. A99, 269 (1967); A99, 289 (1967).
[17] S. A. A. Zaidi and S. Darmodjo, Phys. Rev. Letters 19, 1446 (1967).
[18] R. O. Stephen, Nucl. Phys. A94, 192 (1967).
[19] S. Darmodjo, thesis, University of Texas at Austin, 1968 (unpublished).
[20] H. L. Harney, thesis, Heidelberg, 1968 (unpublished).

the proper choice of optical parameters and the validity of this assumption have been discussed in great detail. According to the Lane equations which connect the nC, pC, and nA systems, the main optical parameters are the well depth $V_n(r)$ which binds the parent analog states, the optical-model potential $V_p(r)+iW(r)$ for proton scattering, and the charge-exchange potential $U_1(\mathbf{t}\cdot\mathbf{T}_0)$. The real parts of these potentials are related through the equation[20,21]

$$T_0U_1(r)+V_p(r)=V_n(r). \quad (5)$$

In principle, all potentials in Eq. (5) can be measured independently: U_1 is taken from the (p,n) cross section or the splitting of isobaric analog and anti-isobaric analog states, V_p+iW is determined from elastic scattering off-resonance angular distributions, and V_n is adjusted so that the experimental binding energies in the nC system are reproduced. It was found that Weidenmüller's theory with $V_p=V_n$ gives an unrealistic background cross section. In the present analysis $S_{cc'}{}^{\rm opt}$ refers to the actual proton potential that fits the off-resonance cross section.

Compared with the "ideal" case of a doubly magic core, e.g., ^{208}Pb, where Eq. (5) could be verified for many isobaric analog states,[17] one faces in ^{90}Zr a more complex situation. For most low-lying states in ^{90}Zr the simple shell-model description of two $p_{1/2}$-$g_{9/2}$ protons built onto the ^{88}Sr ground state[22] seems to work successfully. Even the ground state is known to have a mixed $(p_{1/2})^2$-$(g_{9/2})^2$ proton configuration,[23,24] which indicates a nearly degenerate $p_{1/2}$ and $g_{9/2}$ single-particle energy and the lack of a pronounced $p_{1/2}$ subshell structure.[25] From an analysis of the ^{90}Zr$(d,p)^{91}$Zr stripping data, a fairly large fractionization of the $s_{1/2}$, $d_{3/2}$, and $g_{7/2}$ neutron strengths[3] has been found. The "centers of gravity" of the $d_{3/2}$ and $g_{7/2}$ strength are shifted by 700 and 500 keV, respectively, against the strongly populated state. Consequently, the neutron potential $V_n(r)$ of the nC system is only roughly fixed. Besides these facts which make the choice of ^{90}Zr as a "good" core questionable, there are hints from inelastic proton scattering[4] and the ^{91}Zr(d,t) reduced widths[3] that at least the second 0^+ state in ^{90}Zr can be regarded as a "good" core state. A discussion of this point is given in Sec. 3 B. Finally, because of the (p,n) threshold at 7.56 MeV and the low bombarding energy, the optical parameters $V_p(r)+iW(r)$ describing the elastic proton scattering are expected to change appreciably over the energy range of the excitation functions.

TABLE II. Optical parameters for the nC ^{91}Zr system. $R_0=1.23$ F, $a_0=0.60$ F, $R_c=1.20$ F.

			Binding energy (MeV)		
l_j	V_n (MeV)	V_{so} (MeV)	Calculated	Expt.[a]	"Center of gravity"[a]
$d_{5/2}$	51.5	6.25	7.38	7.21	7.18
$s_{1/2}$	52.0	6.25	6.00	6.00	5.63
$d_{3/2}$	51.5	6.25	5.17	5.17	4.48
$g_{7/2}$	49.5	7.00	4.98	5.02	4.48

[a] Reference 3.

The first step of the analysis was to find adequate optical-model-potential parameters for the nC system, i.e., the well depth V_n, radius r_0, diffuseness a_0, and spin-orbit potential V_{so} of a real Woods-Saxon potential which give the correct binding energies of the $d_{5/2}$ ground state, 1.21-MeV $s_{1/2}$ and 2.04-MeV $d_{3/2}$ state in ^{91}Zr. A computer code BEMAIN written by T. Tamura was used to calculate the well depth V_n for given neutron-binding energies, V_{so} and the geometrical quantities r_0 and a_0. The set of "best" parameters is listed in Table II. Since the $g_{7/2}$ state always turned out to be too strongly bound, its well depth was lowered but without changing the geometry.

Next we fitted the background of the elastic scattering excitation curves and the off-resonance angular distributions at 6.35, 6.898, and 8.384 MeV. In addition to the data given in Sec. 2 we included previously measured excitation functions at the 6.8-MeV $d_{3/2}$ resonance[26] and fits to off-resonance angular distributions at 5.68, 6.35, and 7.112 MeV.[12] For fitting the angular distributions we used the program PEREY[27] with a surface type imaginary potential W_D. The fits are shown in Fig. 7. One has to notice that the cross sections at forward angles are missing and that effects from neighboring resonances cannot be excluded. Because of the known uncertainties of the optical model at low energies we searched only for V_p, W_D, and the diffuseness of the imaginary potential. The energy dependence of these parameters is summarized in Table III and Fig. 11(b) with values from proton scattering on ^{90}Zr and ^{91}Zr at higher energies included. The sudden rise of W_D near 7.5 MeV is thought to reflect the (p,n) threshold (see Sec. 2 D).

Using these energy-dependent optical parameters we fitted the elastic scattering excitation functions by means of the code JULIUS described in Ref. 19. The resonance parameters are listed in Table V. The single-particle widths $\Gamma_{lj}{}^{(\rm sp)}$ listed also in Table V were calculated by means of the computer code GPMAIN written by S. A. A. Zaidi. This program computes the matrix element $\langle\phi_{nA}|U_1|\phi_{pC}{}^{(+)}\rangle$ of Eq. (3) using the bound-state wave functions obtained from BEMAIN and the real volume-type charge-exchange potential

$$U_1(r)=U_1\{1+\exp[-(r-R_0)/a]\}^{-1}.$$

[21] T. Tamura (private communication).
[22] J. Vervier, Nucl. Phys. **75**, 17 (1966).
[23] J. B. Ball, in Proceedings of the International Conference on Nuclear Structure, Tokyo, 1967, p. 69 (unpublished).
[24] B. M. Freedom, E. Newman, and J. C. Hiebert, Phys. Rev. **166**, 1156 (1968).
[25] V. Gillet, B. Giroud, and M. Rho, Nucl. Phys. **A103**, 257 (1967).
[26] G. Terrell, C. F. Moore, J. L. Adams, and D. Robson, *Proceedings of the Conference on Isobaric Spin in Nuclear Physics, Tallahassee, Florida* (Academic Press Inc., New York, 1966), p. 382.
[27] F. J. Perey, Phys. Rev. **131**, 745 (1963).

TABLE III. Optical parameters for elastic proton scattering on ^{91,90}Zr searched by PEREY.

Reaction	Energy (MeV)	V_p (MeV)	a_r (F)	W_D (MeV)	a_i (F)	V_{so} (MeV)	a_{so} (F)	R (F)	R_c (F)	Ref.
^{90}Zr+p	5.68									a
	6.35	57.5	0.60	1.25	0.70	5.50	0.65	1.25	1.25	
	7.11									
	6.35	56.6	0.60	0.15	0.75	6.25	0.65	1.23	1.20	b
	6.90	56.2	0.60	0.39	0.90	6.25	0.65	1.23	1.20	
	8.38	55.4	0.60	5.88	0.68	6.25	0.65	1.23	1.20	
	12.70	52.6	0.64	6.00	0.763	7.90	0.65	1.235		c
	18.80	52.0	0.70	9.25	0.65	6.20	0.65	1.20		d
^{91}Zr+p	14.8	52.7	0.60	9.35	0.65	5.50	0.65	1.22	1.22	e

[a] Reference 12.
[b] Present work.
[c] J. K. Dickens, E. Eichler, and G. R. Satchler, Phys. Rev. 168, 1355 (1968).
[d] Reference 31.
[e] L. S. Michelman (private communication).

We choose the same geometry, $R_0=1.23A^{1/3}$ F and $a=0.60$ F, as for the nC system. The well depth $U_1=1.0$ MeV was obtained from Eq. (5) by setting $V_p=56.5$ MeV, $V_n=51.5$ MeV, and $T_0=5$.

B. Inelastic Scattering Channels

1. General Remarks

Before going into a quantitative analysis some features common to all inelastic channels are mentioned:

(1) Each channel exhibits 7–12 resonances in the range of 4.5–9.5 MeV bombarding energy superimposed on a flat background which has a broad maximum near 7.5 MeV.

(2) Resonances in the p_0(g.s.), p_1 (0^+) and p_2 (2^+) channel are strongly correlated in position and total width to each other, and to their parent analog states. However, some resonances in the p_3 (5^-), p_4 (3^-), and p_5 (4^-) channel are shifted in energy or not seen at all in the p_0 channel or in the (d,p) reactions.

(3) For each inelastic group p_i there exists at least one pronounced resonance near $E_{p_i}=E_{p_0}(d_{5/2})-Q_i$ where $E_{p_0}(d_{5/2})=4.63$ MeV denotes the c.m. energy of the lowest ground-state $d_{5/2}$ resonance and Q_i is the Q value of the excited state. Assuming an extreme weak-coupling model, E_{p_i} is the theoretical c.m. bombarding energy of the lowest $d_{5/2}$ resonance in channel i.

(4) Similar results have been recently obtained in proton scattering experiments on the neighboring $N=50$ targets ^{88}Sr,[28] ^{89}Y,[29] and ^{92}Mo.[30]

2. 1.75-MeV p_1 Channel

Three strong and at least six minor resonances occur in the excitation function of the p_1 group (Fig. 3). From their position the pronounced resonances have been identified with the $d_{5/2}$, $s_{1/2}$, and $d_{3/2}$ isobaric analog states weakly coupled to the first excited 0^+ state.[4] Following the weak-coupling idea, the absolute cross section, angular distributions, and resonance shapes will be discussed in more detail in this section.

According to Weidenmüller's theory [Ref. 16, Eq. (4.1)] the inelastic scattering cross section is the sum of a resonance term $\sigma_{cc'}{}^{\rm res}\propto|\langle S_{cc'}\rangle|^2$, a modified background part $\sigma_{cc'}{}^{\rm int}$ including the interference of the isobaric analog state with the $T_<$ states having the same spin and parity as the resonance, and a Hauser-Feshbach term $\sigma_{cc'}{}^{\rm HF}$ describing the reaction through $T_<$ states with different spin and parity. In the case where both initial and final state have $J^\pi=0^+$, $\sigma_{cc'}$ has the form

$$\sigma_{cc'}=\pi\lambda_p{}^2g^J[|\langle S_{cc'}\rangle|^2+T_J(E)T_J(E-Q_1)/\sum_{c''}T(E-Q_{c''})]+\pi\lambda_p{}^2\sum_{lj}{}'\,g^jT_{lj}{}^{\rm HF}(E)T_{lj}{}^{\rm HF}(E-Q_1)/\sum_{c''}T(E-Q_{c''}),\quad(6)$$

where J denotes the spin of the resonance, Q_1 the Q value of the final state, and the sum $\sum_{c''}T(E-Q_{c''})$ is extended over all open channels. The transmission factors T_J have been taken from Eqs. (3.4), (3.5), and (4.6) of Ref. 16. The prime of the Hauser-Feshbach sum excludes the contribution with $j=J$. The coherent direct-reaction part $S_{cc'}{}^0$ has been neglected since the 90° symmetry of most angular distributions indicates a rather pure compound-nuclear reaction mode and since the direct-reaction cross section at 18.8 MeV has been found to be very small.[31,32]

Outside the resonance all transmission coefficients $T_{lj}=1-\sum_{c''}|\langle S_{cc''}\rangle|^2$ are given by their Hauser-Feshbach values

$$T_{lj}{}^{\rm HF}=4Y_{lj}/(1+Y_{lj})^2,\quad(7)$$

which have been obtained from the computer code PEREY[27] using the energy-dependent absorptive potential $W_D(E_p)$ given in Fig. 11(b).

[28] E. R. Cosman, J. M. Joyce, and S. M. Shafroth, Nucl. Phys. A108, 519 (1968).
[29] D. D. Long and J. D. Fox, Phys. Rev. 167, 1131 (1968).
[30] P. Richard and C. Ling (private communication).
[31] W. S. Gray, R. A. Kenefick, J. J. Kraushaar, and G. R. Satchler, Phys. Rev. 142, 735 (1966).
[32] M. B. Johnson, L. W. Owen, and G. R. Satchler, Phys. Rev. 142, 748 (1966).

In Fig. 11(c) the experimental background reaction cross section summed over the inelastic channels taken from the excitation functions and angular distributions is compared with the Hauser-Feshbach estimate $\sum_{p'} \sigma_{pp'}{}^{\mathrm{HF}}(E)$. We assumed that below the neutron threshold energy only the elastic channel and the inelastic channels below 4-MeV excitation energy contribute to the sum $\sum_{c''} T_{c''}(E-Q_{c''})$. Above 7.5 MeV the background in all inelastic channels decreases slowly because of the additional term $\sum_n T_n$ in the denominator. (Recent measurements of the ^{92}Mo(p,p') reaction[30] are in line with this explanation. Here, the background still keeps increasing at $E_p=8.5$ MeV, which is below the (p,n) threshold at 9.08 MeV.)

Because of the many constants entering Eq. (6) and the peculiar form of the transmission factors $T_J(E)$, the cross section $\sigma_{cc'}$ is a complicated function of energy over the resonance, and an analysis of the many-channel case, for example the $s_{1/2}$ resonance at 7.34 MeV, is not encouraging. However, at least the $d_{5/2}$ resonance at 6.28 MeV suggests an easy explanation for the following reasons: (1) This resonance is only weakly seen in all proton channels except the p_1 group. (2) Its energy lies below the neutron threshold. (3) In the ^{90}Zr(d,p) reaction the neutron spectroscopic factor of the parent analog state[3] was found to be very small ($S_n=0.029$). (4) The spectroscopic factor measured in the pickup reaction ^{91}Zr$(d,t)^{90}$Zr (1.75 MeV, 0^+) also turned out to be small ($S_{d,t}=0.005$).[3] From (3) and (4), Cohen and Chubinski[3] concluded that the orthogonality of the ^{90}Zr ground and first excited state pertains also in the nC system. Making the same assumption for the pC system is justified by the fact that our data do not show the 6.28-MeV resonance in the elastic channel. Neglecting the decay into other inelastic channels, one is left again with a two-channel case. The resonance is mainly populated through isospin mixing in the entrance channel and decays according to its "natural" weak-coupling structure. Therefore, the reaction is similar to an inverse (p,n) reaction, where the isospin-forbidden part is known to occur in the exit channel.

TABLE IV. Angular distribution coefficients B_L for inelastic proton scattering through an IAR for $J_{\mathrm{initial}}=J_{\mathrm{final}}=0^+$ and $J_{\mathrm{IAR}}=J$. The notation used was

$$W(\theta)=1+\sum_{L=2}^{2J-1} B_L P_L(\theta).$$

(a) Theoretical coefficients B_L

J	B_2	B_4	B_6
$\frac{1}{2}$			
$\frac{3}{2}$	1.000		
$\frac{5}{2}$	1.142	0.857	
$\frac{7}{2}$	1.190	1.051	0.758

(b) Experimental coefficients B_L

Energy (MeV)	Weak-coupling state	J^π	B_2	B_4
6.283	$0_2{}^+ d_{5/2}$	$\frac{5}{2}^+$	0.90±0.06	0.42±0.07
6.352	off		0.46±0.06	0.25±0.08
6.766	off		0.60±0.04	0.06±0.05
6.843	$0_1{}^+ d_{3/2}$	$\frac{3}{2}^+$	0.66±0.03	0.01±0.03
6.898	off		0.60±0.03	0.01±0.03
7.343	$0_2{}^+ s_{1/2}$	$\frac{1}{2}^+$	0.34±0.05	0.12±0.06
7.896	$2^+ s_{1/2}$	$\frac{3}{2}^+$	0.68±0.04	0.17±0.06
8.031	off		0.70±0.03	0.01±0.03
8.119			0.63±0.03	0.02±0.03
8.384	off		0.60±0.04	0.08±0.05
8.506	$0_2{}^+ d_{3/2}$	$\frac{3}{2}^+$	1.00±0.03	0.17±0.05

Before going into the details of the fitting procedure one has to estimate the nonresonant Hauser-Feshbach term $\sigma_{cc'}{}^{\mathrm{HF}}$. This has been done by analyzing the p_1 angular distributions. As has been pointed out, most angular distributions of the p_1 group, on and off the resonance, are nearly symmetric about 90°, supporting a compound-nuclear reaction. Theoretical expressions for the differential cross section in the jj-coupling scheme (which is most suitable for proton scattering via an isobaric analog resonance) have been given by Robson.[33] Remembering the "giant resonance" structure of the IAR, one expects $\sigma_{cc'}{}^{\mathrm{res}}$ and $\sigma_{cc'}{}^{\mathrm{int}}$ to have the same angular dependence. In the case $J_{\mathrm{initial}}=J_{\mathrm{final}}=0^+$, $J=J_{\mathrm{IAR}}$, the angular distributions of $\sigma_{cc'}{}^{\mathrm{res}}+\sigma_{cc'}{}^{\mathrm{int}}$ can be written as[29,31,34]

$$W(\theta)=\sum_{L=0}^{2J-1} B_L P_L(\theta),$$

$$B_L=\tfrac{1}{4}(2J+1)^4(2L+1)\begin{pmatrix} J & J & L \\ \frac{1}{2} & -\frac{1}{2} & 0 \end{pmatrix}^2 \begin{Bmatrix} J & J & L \\ J & J & 0 \end{Bmatrix}^2. \quad (8)$$

The theoretical coefficients B_L for $J=\frac{1}{2},\frac{3}{2},\frac{5}{2},\frac{7}{2}$ are listed in Table IV(a). Since their magnitude is near unity they allow an unambiguous spin assignment of the resonance by looking at the highest term B_{2J-1}. In Table IV(b) the measured B_L coefficients on and off resonance are compared with the prediction of Eq. (8). The agreement is fairly good, especially for the $d_{3/2}$ resonance. The strong P_4 term in the 6.28-MeV resonance determines its spin to be $J=\frac{5}{2}$ as has been suggested previously.[4]

Since each angular distribution was found to be given by the three parameters B_0, B_2, and B_4 it was possible to deduce the energy dependence of the B_2 coefficients from the measured excitation functions. The result is shown in Fig. 12. The fitting curves to the absolute cross sections have been obtained from the program PRIM, which computes Eq. (6) with the spectroscopic factors and $(\Delta^{(sp)}/\Gamma^{(sp)})$ as parameters. The nonzero target thickness has been taken into account. The parameters are listed in Table V. Since the $d_{5/2}$ and $d_{3/2}$ resonances do not appear in the elastic channel, only upper limits for the incoming channel widths and lower limits for the widths in the exit channels could be found.

The absolute cross sections show fairly symmetric resonance shapes. For the $s_{1/2}$ and $d_{3/2}$ resonance this

[33] D. Robson, in *Proceedings of the Symposium on Recent Progress in Nuclear Physics with Tandems*, edited by W. Hering (Max Planck Institute for Nuclear Physics, Heidelberg, 1966).

[34] E. Sheldon and D. M. van Patter, Rev. Mod. Phys. 38, 143 (1966).

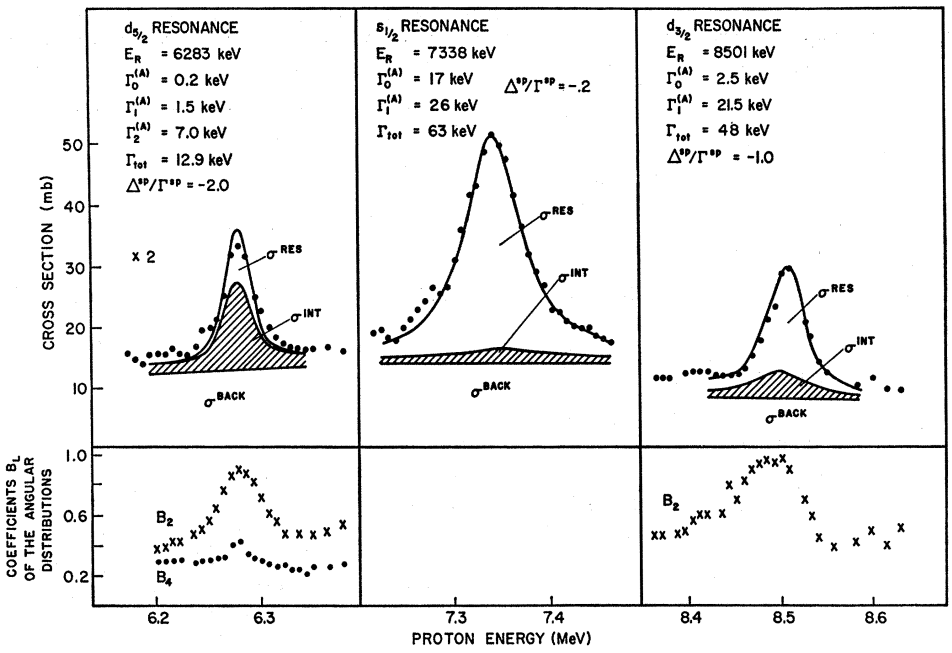

FIG. 12. Weak-coupling resonances in the p_1 (0_2^+) channel, the fitting parameters are listed in Table V; the energy dependence of the B_2 and B_4 coefficients is given below.

can be explained by the many inelastic proton and/or neutron channels. They damp the asymmetry[16] predicted for the two-channel case.[18,35,36] The $d_{5/2}$ resonance, on the other hand, is expected to have an asymmetric shape. Unfortunately, the target thickness in this resonance was 20 keV and exhausts most of the total width $\Gamma = 36$ keV. Hence, even a large asymmetry would be smeared out. A more refined study of this resonance using a very thin target is in progress.

3. 2.18-MeV p_2 Channel

The excitation functions of the p_2 (2^+) group (Fig. 4) exhibit several strong resonances between 6.7 and 8.6 MeV. Their energies listed in Table VI agree well with the resonance energies found in the p_0 (0^+) and p_1 (0^+) channels. In extracting the partial and total widths (Table V) the interference term $\sigma_{cc'}^{int}$ in Eq. (6) has been neglected.

TABLE V. Resonance parameters in the ^{90}Zr+p systems compared with spectroscopic factors in the ^{90}Zr+n systems.

^{90}Zr+n										
E_x (MeV)	1.48	1.89	2.06	2.21	2.58	2.88	3.11	3.30	3.49	3.70
l_j	$d_{3/2}$	$g_{7/2}$	$d_{3/2}$	$g_{7/2}$	$s_{1/2}$	$d_{3/2}$	$d_{3/2}$	$d_{3/2}$	$g_{7/2}$	$d_{3/2}$
S_n	0.029	0.06	0.45	0.52	0.24	0.078	0.105	0.15	0.33	0.10
^{90}Zr(p,p_0) g.s.										
E_R^{lab} (MeV)			6.860	7.060	7.339	7.703	7.910	8.103		
Γ (keV)			60	27	80	65	50	50		
$\Gamma_0^{(A)}$ (keV)	$\leq$1.0		15	2.5	17±3	10	8	8		$\leq$5
$\Gamma_0^{(sp)}$ (keV)	12.8		39.3	3.2	71.6	44.4	46.0	47.3		50.1
S_0	$\leq$0.08		0.38	0.78	0.24±0.04	0.22	0.18	0.15		$\leq$0.10
^{90}Zr(p,p_1)1.75										
E_R^{lab} (MeV)	6.283(5)[a]		6.848(5)	6.848(5)	7.338(5)[a]	7.674(5)	7.889(5)	8.137(5)		8.501(5)[a,b]
l_j	$d_{5/2}$		$j\leq\frac{3}{2}$		$s_{1/2}$			$j\leq\frac{3}{2}$		$d_{3/2}$
Γ (keV)	12.9±1.5		50±5		63±5	40±10	42±8	56±5		48±5
$\Gamma_1^{(A)}$ (keV)	$\geq$1.1		1.9		26±7	1.6	4.4			$\geq$8
$\Gamma_1^{(sp)}$ (keV)	3.8		30	55	55	35.4	36.4	37.5		39.0
S_1	$\geq$0.29		0.07		0.47±0.13	0.05	0.12			$\geq$0.2
^{90}Zr(p,p_2)2.18										
E_R^{lab} (MeV)	6.274		6.848	7.063	7.347	7.700	7.894		8.318	8.502
Γ (keV)			54±2	28±2	61±8	40±5	47±2		28±2	67±8
$\Gamma_2^{(A)}$ (keV)	$\geq$4.8		4.1	2.6	9.3	6.4	15			$\geq$12

[a] The parameters for the best fits are displayed in Fig. 12.
[b] The sum of the neutron transmission coefficients $\Sigma_n T_n = 6.1$ was calculated from Table IX, W. S. Emmerich, in *Fast Neutron Physics II* edited by J. B. Marion and J. L. Fowler (Interscience Publishers, Inc., New York, 1963), p. 1097.

[35] D. Robson, Phys. Rev. **137**, B535 (1965).
[36] R. Lipperheide, Nucl. Phys. **A105**, 545 (1967).

TABLE VI. Resonance energies in keV in the $^{90}Zr+p$ system.

p_0 (ground state)	p_1 (1.75 MeV)	p_2 (2.18 MeV)	p_3 (2.32 MeV)	p_4 (2.75 MeV) 3^-	p_5 (2.75 MeV) 4^-
	6283±5[a]	6274±5			
6520±10					
		6709±5			
6860±10[a]	6848±5	6848±5	6810±7		
					6935±7
			7014±5		7013±5
7060±10[a]		7062±5[a]			
			7188±5		
7339±10	7338±5[a]	7347±5	7347±5[a]	7353±5[a]	7353±5[a]
					7420±7[a]
				7583±5[a]	
	7674±5		7646±5		
7703±10		7700±5[a]			
					7790±5[a]
7910±10	7889±5	7894±5[a]			
8103±10		8119±5			
				8266±5	
8316±10		8295±5	8306±5[a]		
	8501±5[a]	8502±5		8367±10	
				8630±10[a]	
		8844±7			
			8961±7	8947±10[b]	
		9130±7	9138±7	9126±10[b]	
			9317±5[a]	9300±10[b]	
				9377±10[b]	

[a] Strong resonances.
[b] No unique assignment could be made.

A survey of the possible reaction types that can excite the 2^+ state in ^{88}Sr has been given by Cosman *et al.*[29] Recently, Auerbach[2] obtained qualitative agreement on ^{88}Sr assuming that only the $\phi_c{}^{2+}\pi(l_j)$ weak-coupling part [Eq. (2)] of the analog resonances accounts for the p (2^+) cross section. Compared with ^{88}Sr the strength in the p (2^+) channel in ^{90}Zr is distributed over more resonances. This is expected from the fractionization of the single-particle strengths found in $^{90}Zr(d,p)$ and $^{90}Zr(p,p_0)$, and the intimate connection of the proton configurations of the ground state and the lowest two excited states. Indications for the validity of the weak-coupling model are the isotropic angular distribution of the strong 7.894-MeV resonance which favors a $[\phi_c{}^{2+}\pi(s_{1/2})]_{J^\pi=3/2^+}$ configuration and a strong $J^\pi=\frac{3}{2}^+$ resonance at 6.848 MeV, where the "center of gravity" of the $\phi_c{}^{2+}\pi(d_{5/2})$ resonances is expected. However, no attempt has been made to analyze the angular distributions of the other resonances.

4. 2.32-MeV 5^- State and 2.75-MeV 3^-, 4^- States

A qualitative discussion of our results for the 3^-, 4^-, and 5^- inelastic proton groups is lead by the weak-coupling model discussed above and by the situation found in ^{208}Pb for the corresponding states. There, only one pronounced resonance at 14.9 MeV occurs in the inelastic scattering cross section of the p (4^-) and p (5^-) groups.[6,37] This peak has been explained by "recoupling" the angular momenta of the neutron-hole neutron part of the 2p–1h configuration

$$\pi(g_{9/2})[\nu(g_{9/2})\nu^{-1}(p_{1/2})]_{J^\pi=4^-,5^-}.$$

Because of the collective nature of the 3^- state the p (3^-) group, on the other hand, resonates at several energies.

In ^{90}Zr and in ^{92}Mo (Ref. 30) the number of resonances in the p (4^-) group is nearly the same as in the p (3^-) channel and the resonance cross sections to the lowest negative-parity channels in ^{88}Sr, ^{90}Zr, and ^{92}Mo have the same magnitude of 5–15 mb. About half of the resonances coincide with positive-parity resonances in the elastic and the p (2^+) channel, others are shifted up to 100 keV or were not detected at all in the elastic scattering excitation functions, nor were their parent analog states in the $^{90}Zr(d,p)$ reaction detected.

From the many reaction types quoted by Cosman *et al.*[28] none is favored to account for the fairly large cross sections to the negative-parity states. From the shell model one expects an $l_j=s_{1/2}, d_{3/2}, d_{5/2}$, or $g_{7/2}$ proton coupled to the negative-parity core state. This gives rise only to negative-parity resonances in contrast to the positive partial waves in the incoming channel. The main 2p–1h part of the IAR, on the other hand, is

$$\{[\pi(g_{9/2})\nu^{-1}(g_{9/2})]_0\nu(l_j)\}_{J=j},$$

which decays only to positive-parity states. Hence, both main $T_>$ parts of the IAR [see Eq. (2)] do not excite the 3^-, 4^-, and 5^- states.

Most authors discuss the low-lying spectrum ^{90}Zr and ^{92}Mo assuming proton excitations with respect to

[37] C. F. Moore, J. G. Kulleck, P. von Brentano, and F. Rickey, Phys. Rev. 164, 1559 (1967).

an inert ^{88}Sr or ^{90}Zr core[8,22] and assign a $[\pi(g_{9/2})\pi \times(p_{1/2})]_{J^\pi=4^-,5^-}$ configuration to the lowest 4^- and 5^- states in ^{90}Zr and ^{92}Mo. However, measurements of inelastic α scattering[38] and proton scattering cross sections[31,39] suggest that even in exciting the 5^- states, core polarization plays an important role. The strength of the $5^- \rightarrow 0^+$ $E5$ γ-ray transitions, for example, were found to be $\Gamma(E5,^{90}\text{Zr})=3.6$-W.u. and $\Gamma(E5,^{92}\text{Mo})=4.0$ W.u., respectively.[38] Consequently, one may assume that the wave functions of the 4^- and 5^- states have small neutron-neutron hole admixtures. Remembering the strong mixing of the ^{90}Zr ground state, one can excite in an $l_j=g_{7/2}$ resonance the 1p–1h configuration

$$[\nu(g_{7/2})\nu^{-1}(p_{1/2})]_{J^\pi=3^-,4^-},$$

or the 2p–2h configuration

$$[\pi(p_{1/2})\pi(g_{9/2})\nu^{-1}(g_{9/2})\nu(g_{7/2})]_{J^\pi=3^-,4^-},$$

where in both cases the emission of a $p_{1/2}$ proton is strongly favored by its high penetrability.

Some of the resonances not seen in the elastic channel may be due to capturing an $h_{11/2}$ proton, which is expected to occur about 330 keV above the strong $g_{7/2}$ resonance at 7.00 MeV. Below the (p,n) threshold, resonances are also likely to be populated by isospin mixing in the incoming or outgoing channel as has been discussed in Sec. 3 B 2 for the $1.75/d_{5/2}$ resonance. Finally, one may consider protons of the next negative-parity shell coupled to a negative-parity core state forming (pC) configurations of the type

$$[\phi_c{}^{4^-}\pi(f_{7/2})]_{J^\pi=1/2^+},$$

for example.

The discussion given here is admittedly very tentative. However, it seems worthwhile to mention the possibilities that are most compatible with the properties of the ^{90}Zr states and the restrictions from the penetration factors at the low bombarding energy. In a forthcoming paper we shall concentrate on this subject.[40]

4. CONCLUSION

Isobaric analog states in ^{91}Nb were populated by the ^{90}Zr$+p$ reaction. Angular distributions and excitation functions of the elastically and inelastically scattered protons leading to the first excited 0^+ state are analyzed in terms of Weidenmüller's theory,[16] which was modified to give the correct off-resonance background. The change of optical-model parameters because of the opening of the neutron channel was taken into account. The spectroscopic information for several resonances is listed in Table V.

The spins and parities of the three strong resonances found in the p_1 group at 6.28, 7.34, and 8.50 MeV were determined to be $J^\pi=\frac{5}{2}^+$, $\frac{1}{2}^+$ and $\frac{3}{2}^+$, respectively, in agreement with the simple weak-coupling model proposed previously.[4] The agreement between the experimental results in the p_0 (0^+) and p_1 (0^+) channels and the predictions of Weidenmüller's theory are satisfactory. However, this agreement is not thought to give a very sensitive test for the following reasons: Below the (p,n) threshold ($E_p=7.56$ MeV) the Y_{lj} are very small. Hence, the crucial quantity

$$f_{lj}=[\Gamma_{lj}{}^{(A)}/\Gamma_{lj}{}^{p}]^{1/2}=(1+2iY_{lj}\Delta^{(sp)}/\Gamma^{(sp)})(1+Y_{lj})^{-1}$$

connecting the measured partial width $\Gamma_{lj}{}^{p}$ and the IAR partial width $\Gamma_{lj}{}^{(A)}$ is nearly unity. Even drastic changes of $\Delta^{(sp)}/\Gamma^{(sp)}$ do not substantially change the fit in the elastic channel. Above the threshold the resonances in the elastic channel are weak so that the experimental uncertainties do not allow a very sensitive comparison. In the analysis of the p_1 (0^+) channel the influence of the other inelastic channels and the open neutron channel has been only roughly taken into account.

Although, according to their energy position, many strong resonances in the inelastic proton groups due to higher states ($J^\pi=2^+$, 5^-, 3^-, 4^-) are compatible with a weak-coupling model, it was not possible to quantitatively analyze their angular distributions in terms of a pure compound-nuclear reaction.

ACKNOWLEDGMENTS

We wish to thank W. R. Coker, D. Robson, T. Tamura, H. A. Weidenmüller, and S. A. A. Zaidi for helpful discussions and for providing us with some of the computer programs used in the analysis. The help of J. Kulleck and R. Jones in taking the data is much appreciated. We also acknowledge the help and interest of B. M. Foreman in the initial states of the γ work.

[38] E. J. Martens and A. M. Bernstein, Nucl. Phys. **A117**, 241 (1968).
[39] W. G. Love and G. K. Satchler, Nucl. Phys. **A101**, 424 (1967).
[40] K. P. Lieb, T. Hausmann, J. J. Kent, and C. F. Moore, Z. Physik (to be published).